Analysis of an Experimental Technique for Determining Van der Pol Parameters of a Transistor Oscillator

Kuang Yi Chen, Paul D. Biernacki, A. Lahrichi, and Alan Mickelson, *Senior Member, IEEE*

***Abstract*—The Van der Pol (VDP) model of a transistor oscillator describes the behavior of the oscillator with three parameters. When operating in steady state, only two parameters can be determined by spectrum analysis, these being the oscillation frequency and amplitude of oscillation. In this paper, a technique for measuring the other VDP parameter is examined. In this approach, a periodically modulated voltage is added to the bias of the oscillator to perturb the operational state. A theoretical derivation shows that the power spectrum of the perturbed oscillator contains additional information for determination of the other VDP parameter. A simple analytical perturbation formula predicts the oscillator's response to the ramped bias. Our experimental results agree with the analytical perturbation solution and, therefore, this allows one to read off the other VDP parameter from the experimental data. The VDP model allows one to predict the behavior of coupled transistor oscillators more accurately and simply than does the traditional large-signal model of the transistor. This VDP model will simplify oscillator array design since the number of parameters needed to describe each oscillator is reduced from that which would be required using a large-signal circuit model.**

I. Introduction

COUPLED transistor oscillators are one implementation for active phased arrays. The design of such active arrays requires one to analyze and predict the performance of coupled oscillators. In a conventional approach, transistor oscillators are investigated by using large-signal models of MESFET's or high electron-mobility transistors (HEMT's) [1]–[8]. The harmonic-balance technique [9] is often used in these large-signal transistor models for nonlinear microwave circuit designs. These models can predict performance of power monolithic microwave integrated circuit (MMIC) amplifiers and oscillators [10]. However, using computer-aided design (CAD) tool packages to analyze a coupled oscillator array, we are faced with a problem that is not easily solved with current software. That is, the large-signal models of the transistor have many variables. Additionally, since almost all of the variables have nonlinear saturation characteristics and are bias dependent, there is generally no easy way to predict how oscillators will perform if parasitics are introduced or if bias conditions drift. As the number of oscillators in the array increases, the array performance becomes more difficult to analyze, as both the computer time and computational errors increase. Since Van der Pol (VDP) coupled oscillator theory has been recognized as an effective way to describe the performance of a coupled oscillator array, a VDP equation for a single transistor oscillator is used in our modeling. The purpose of this paper is to develop simple experimental techniques to determine the VDP parameters for transistor oscillators. It is the importance of understanding the time-dependent dynamics of oscillator design that motivates use of a VDP model. The VDP model allows the dynamics of an oscillator to be reduced to only three parameters: the resonance frequency, the oscillator Q factor, and the nonlinear saturation coefficient. If, for example, active antenna grid arrays [11] are to be used for beam steering and other radar applications, knowledge of the dynamics enables predictions of how fast an antenna can be steered by an external signal and what bandwidth can be expected using specific transistor elements.

In 1927, Van der Pol investigated the self-sustained triode oscillator. He observed that the saturating characteristic of a triode is the one that is proportional to the cube of the oscillation intensity [12]. Later, the formula $\ddot{x} - (\epsilon - \eta x^2)\dot{x} + \omega_0^2 x = 0$ to describe this type of self-sustained nonlinear oscillation was named the VDP oscillator equation. Since 1927, extensive work in the field of self-sustained oscillators has been carried out by many researchers [13]–[16]. Examples include laser, mechanical, and electrical oscillators. Previous studies have shown that even though different mechanisms govern the self-sustained oscillators, they can be described by the VDP equation, as was deduced by fundamental physical arguments in [17]. In Van der Pol's equation, the parameters are related to the physics of individual oscillators. A quasi-optical oscillator array using the VDP coupled oscillator theory has been analyzed by York [18]. In general, there are two approaches to obtain VDP parameters: numerical or experimental. The numerical approach yields low overall accuracy because it is based on imprecise circuit parameters of the oscillator, which are uncertain in the large-signal limit.

Manuscript received December 30, 1996; revised April 7, 1998. This work was supported by the U.S. Office of Naval Research (ONR) under Grant N00014-92-J-1190 and under Grant N00014-95-I-0494, and the U.S. Army Research Office (ARO) under Grant DAAL-03-92-G-0289 and under Grant DAAH-04-93-G0191.

K. Y. Chen was with the Guided Wave Optics Laboratory and Department of Electrical and Computer Engineering, University of Colorado, Boulder, CO 80309-0425 USA. She is now with Aztek Engineering Inc., Boulder, CO 80301 USA.

P. D. Biernacki was with the Guided Wave Optics Laboratory, Department of Electrical and Computer Engineering, University of Colorado, Boulder, CO 80309-0425 USA. He is now with the Naval Research Laboratory, Washington, DC 20375 USA.

A. Lahrichi and A. Mickelson are with the Guided Wave Optics Laboratory, Department of Electrical and Computer Engineering, University of Colorado, Boulder, CO 80309-0425 USA (e-mail: mickel@schof.colorado.edu).

Publisher Item Identifier S 0018-9480(98)04961-8.

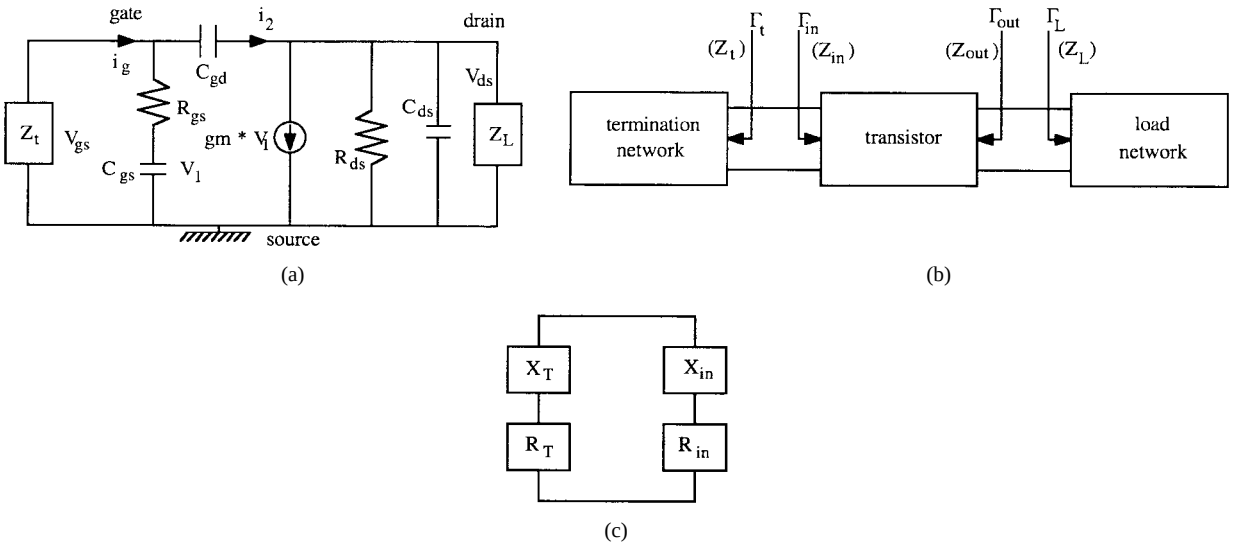

Fig. 1. Three ways of denoting the equivalent circuit model of a common source transistor oscillator. (a) With circuit parameters. (b) As a two-port. (c) As a one-port.

Therefore, in this paper, the experimental approach is used to yield the more accurate parameters to be used in the VDP model. The steady-state solution of the VDP equation contains sufficient information to determine two of the parameters. This paper provides another method to determine the saturation parameter of the transistor oscillator by applying a time-periodic perturbation to the bias voltage of a transistor oscillator. The analysis of the slightly perturbed oscillator is carried out by using a multiple-scale expansion. When a transistor is externally modulated, the sidebands generated in the power spectrum contain the necessary information. Our approach for obtaining the VDP parameters is experimentally verified, and the results agree with the theoretical prediction.

The remainder of this paper is organized as follows. In Section II, we will give an example of how the behavior of the transistor oscillator can be described by the VDP equation. In this example, we will demonstrate that the VDP parameters are directly related to the circuit parameters of the oscillator in a large-signal limit. In Section III, a method for experimentally determining the VDP parameters is derived. From the theoretical derivation and numerical calculations, we show that the VDP parameters which cannot be measured from a steady-state oscillator can be evaluated by the proposed technique. In Section IV, the experimental implementation and results for verifying the theory are discussed. Conclusions are discussed in Section V.

II. VDP Equation for a Self-Sustained Transistor Oscillator

A. Linear-Circuit Model

The feedback mechanism for transistor oscillation can be provided in many different ways. Oscillators can have a common source, common gate, or common drain configurations, and they can have additional capacitance, inductance, or resistance as feedback elements. Even though the physical feedback mechanisms are different, a self-sustained oscillation can be represented by the VDP equation, as Adler so eloquently described in [17]. To demonstrate that the VDP parameters are a function of the circuit parameters of an oscillator and to show how the oscillator circuit can be cast as a VDP oscillator, a radiating oscillator built with a Fujitsu HEMT (fh×35×) is used as a specific example. An equivalent circuit model of an intrinsic MESFET or HEMT [19] is adopted in our modeling. The circuit parameters of the transistor are extracted from the data sheet [20]. The impedance of the source–drain load is represented by the symbol Z_L, and the impedance of the gate–source terminal load is represented by the symbol $Z_{\rm t}$. Both impedances can be calculated from the passive circuit geometry once the main operation mode in the structure is defined. Starting with the small-signal equivalent circuit of Fig. 1 and letting A_0 be the ratio of the alternating voltage drop v_1 in the gate–source capacitor $C_{\rm gs}$ to the gate–source voltage $v_{\rm gs}$, one can write

$$A_0 = \frac{v_1}{v_{\rm gs}} = \frac{1}{j\omega\tau_1 + 1} \tag{1}$$

where $\tau_1 = C_{\rm gs}R_{\rm gs}$. Typically, the value of τ_1 is on the order of 10^{-12}. Since the frequency of our oscillator is in the gigahertz range, A_0 can be approximated to be $A_0 \approx 1$. This then shows, to this order of approximation, that v_1 and $v_{\rm gs}$ are identical. Referring to Fig. 1(a), one sees that this is equivalent to ignoring $R_{\rm gs}$ with respect to $C_{\rm gs}$, an approximation to which we will hold to in what follows.

Defining A_1 as the voltage amplification factor—i.e., A_1 is the ratio of $v_{\rm ds}$ to v_1 (referring to Fig. 1), the following result is obtained:

$$A_1 = -\frac{g_m R_{\rm ds} Z_L}{R_{\rm ds} + Z_L + j\omega C_{\rm ds} R_{\rm ds} Z_L} \tag{2}$$

where it has been assumed that $C_{\rm gd} \ll C_{\rm ds}$. Therefore, the input admittance $Y_{\rm in}$ can be shown to be

$$Y_{\rm in} = j\omega C_{\rm gs} + j\omega C_{\rm gd}\left[1 - \frac{g_m R_{\rm ds} Z_L}{R_{\rm ds} + Z_L + j\omega C_{\rm ds} R_{\rm ds} Z_L}\right] \tag{3}$$

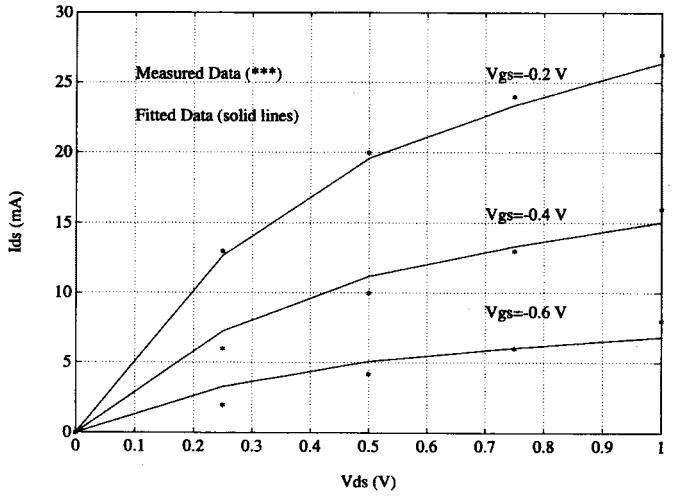

Fig. 2. The I–V curves of the HEMT fh×35×.

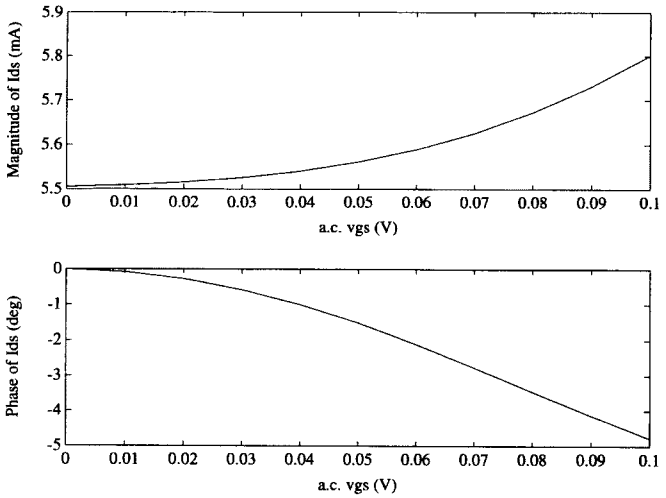

Fig. 3. The effect of the amplitude of ac gate–source voltage on direct drain–source current in the channel.

where, as in (2), $C_{\rm gd}$ is ignored in comparison with $C_{\rm ds}$. However, one cannot ignore $C_{\rm gd}$ completely, as it is the element which provides feedback from output loop to input loop. This feedback is what allows oscillation. Once $C_{\rm gd}$ has been taken into account in the determination of the input impedance, it need not be taken into account again. It is the smallest value of the elements of the circuit and need only be included to first order. Following a similar discussion made by Sevin [21], it can be seen from (3) that if Z_L is either purely resistive or capacitive, the input impedance $Z_{\rm in}$ has a positive resistance and the transistor is stable. However, when Z_L is inductive, the input impedance can have negative resistance and the transistor is unstable, as can be seen from the expression in (3), when a Z_L of $j\omega L$ is substituted, to obtain

$$Y_{\rm in} = j\omega C_{\rm gs} + j\omega C_{\rm gd}\left[1 - \frac{j\omega g_m R_{\rm ds} L}{R_{\rm ds}(1-\omega^2 L C_{\rm ds}) + j\omega L}\right]. \quad (4)$$

Substituting $Z_L = j\omega L_L$ into (2), we observe that the transistor can be unstable, i.e., $|A_1|$ can be greater than one, at the same time that the phase of A_1 can be close or equal to 180°. This is exactly the case for positive feedback. Although $C_{\rm gd}$ may be small and, therefore, the quantity of positive feedback to the input loop small it is unstable. An important observation is that this measured phase relationship of the transistor in the unstable region agrees with previous optical sampling measurements on this radiating oscillator [22]. Oscillation initiates inside the transistor when the magnitude of the negative resistance is larger than the termination impedance. As the intensity of the oscillation increases, the effects of nonlinear components in the circuit will govern the saturation characteristics of the transistor oscillation, forcing the oscillation to reach the steady state. It is these nonlinear bias-dependent saturation characteristics that can be determined and cast into a qualitatively more fundamental formalism which uses the VDP model.

B. Saturation of a Radiating Oscillator

To reach steady-state oscillation, an oscillator must have a nonlinear feedback element. In our case, this element is the transistor. The I–V curve of the fh×35× is shown in Fig. 2. The purpose of this section is to show how the nonlinear-circuit elements eventually can be replaced with the VDP equation. For the HEMT, the advanced Curtice model [1]–[3] is used to fit the curves at different gate–source voltages. In the transistor model, g_m, $C_{\rm gd}$, $C_{\rm gs}$, and $C_{\rm ds}$ are nonlinear and bias dependent. However, if we assume that the main nonlinear element contributing to the saturation is the transconductance g_m, we can calculate the dependence of g_m on the ac gate voltage. The Curtice model describes the drain current with respect to the drain–source and gate–source voltages as

$$I_{\rm ds}(V_{\rm gs}, V_{\rm ds}) = \beta(V_{\rm gs} - V_{\rm ds})^{\kappa}(1 + \lambda V_{\rm ds})\tanh(\alpha V_{\rm ds}) \quad (5)$$

where also

$$g_m = \frac{dI_{\rm ds}}{dV_{\rm gs}}. \quad (6)$$

Values of parameters β, κ, λ, and α are obtained from nonlinear fitting of the I–V curves and are bias independent. The dc bias conditions of our oscillator are $V_{\rm gs} = -0.6$ V and $V_{\rm ds} = 0.6$ V. As the oscillator begins oscillation at frequency ω with ac voltage amplitudes $v_{\rm gs}$ and $v_{\rm ds}$, the voltages $V_{\rm gs}$ and $V_{\rm ds}$ in (5) become

$$V_{\rm gs} = V_{\rm gs\,dc} + v_{\rm gs}\cos(\omega t) \quad (7)$$

$$V_{\rm ds} = V_{\rm ds\,dc} + v_{\rm ds}\cos(\omega t + \phi). \quad (8)$$

By substituting (7) and (8) along with fitting parameters α, β, and λ into (5), and expanding the terms in the frequency variable ω, $I_{\rm ds}$ becomes the superposition of the following terms:

$$I_{\rm ds} = I_{\rm ds0}(\omega^0) + I_{\rm ds1}(\omega) + I_{\rm ds2}(2\omega) + \cdots \quad (9)$$

where $I_{\rm ds0}$ is the component of the dc current in the channel. Fig. 3 shows the relationship of the magnitude of the dc current $I_{\rm ds}$ versus the magnitude of the alternating voltage $v_{\rm gs}$. It can be seen that as $v_{\rm gs}$ increases, $I_{\rm ds}$ increases. The drift of the dc bias voltage $\Delta V_{\rm gs}$ due to the change of dc current can be calculated as follows:

$$\Delta V_{\rm gs} = \frac{I_{\rm ds} - I_{\rm ds\,dc}}{g_{m\,\rm dc}}. \quad (10)$$

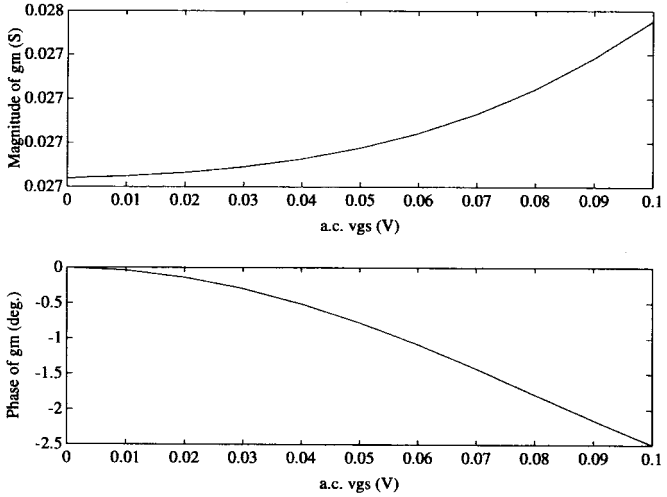

Fig. 4. The effect of the amplitude of ac gate–source voltage on transconductance from the nonlinear computation.

In (10), $g_{m\,\mathrm{dc}}$ is the transconductance at the original bias point. Notice that all the circuit components of the transistor are bias dependent. However, the sensitivity to the change of the voltages is different from component to component. It has been shown that transconductance is the main gain mechanism of the HEMT and is also the most nonlinear component in the transistor [19], [21]. The relationship of the transconductance g_m with respect to ac voltage amplitude v_{gs} can be computed directly from (6) to (10). Their relationship is shown in Fig. 4.

The effect of the bias dependence of gate–source capacitance C_{gs} on oscillation has also been studied. The results of the calculation indicate that the capacitance C_{gs} plays the role of positive feedback and the transconductance g_m plays the role of negative feedback in our oscillator. Since the saturation effect is the main consideration in the investigation (i.e., we only consider the case where the oscillator will reach the steady state), we conclude that the main effect of nonlinearity is indeed from the transconductance. Fig. 4 shows that the value of the transconductance is increased as the ac voltage v_{gs} increases. The VDP oscillator equation can be derived in a rather straightforward manner. Referring to Fig. 1(b), for oscillator design we define

$$Z_{\mathrm{in}} = R_{\mathrm{in}} + jX_{\mathrm{in}} \tag{11}$$

and

$$Z_T = R_T + jX_T = R_T + \frac{1}{j\omega C_T} \tag{12}$$

where, for simplicity, we have assumed that our input termination consists of a series R_T and C. The effect of the amplitude of ac voltage on the input resistance and the input reactance of the transistor is shown in Fig. 5(a) and (b). Their relationship can be fit into the simple form

$$R_{\mathrm{in}} = -R_{\mathrm{in0}} + m_{\mathrm{in}} v_{\mathrm{gs}}^2 \tag{13}$$

where R_{in0} is the initial input resistance of the transistor and m_{in} is the fitting parameter. When the magnitude of R_{in0} is larger than the load resistance, the amplitude of the oscillation increases. As a result, the negative input resistance decreases

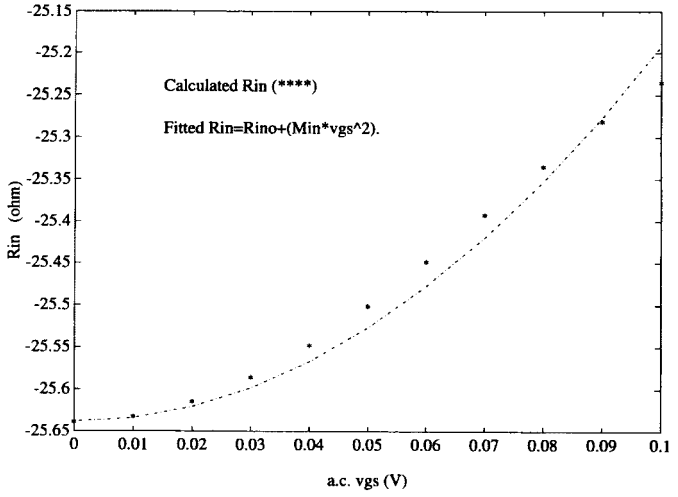

(a)

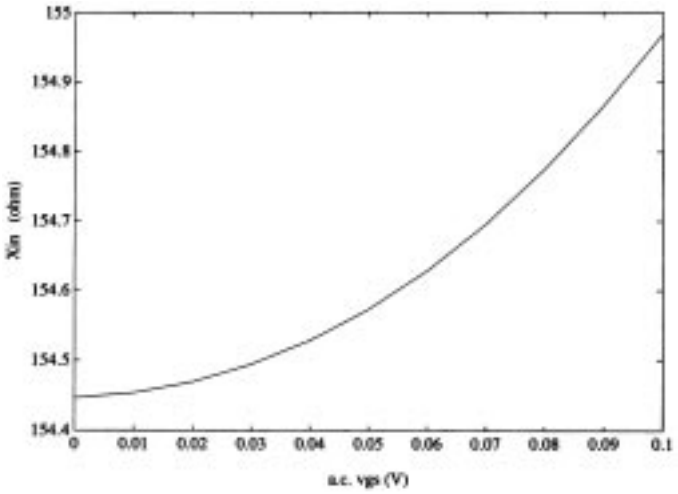

(b)

Fig. 5. The effect of the amplitude of ac gate–source voltage on the (a) input resistance and (b) input reactance of the transistor.

[as shown in Fig. 5(a)]. Eventually, when the magnitude of the negative resistance equals the load resistance, the oscillation reaches a steady state. Fig. 5(b) shows that the input reactance X_{in} is inductive in our oscillator. The value of the reactance also changes with the amplitude of the oscillation. To derive an equivalent VDP model for the transistor oscillator, we can assume that L and C_T are fixed within the frequency range of operation. The equation describing the circuit becomes

$$\frac{L\,di}{dt} + (R_T + R_{\mathrm{in}})i + \frac{1}{C_T}\int i\,dt = 0. \tag{14}$$

Since C_{gd} is small [23] and we have already taken it into account in the Z_{in} calculation, we can ignore its effect on the current $i(t)$. In this limit, the current $i(t)$ is roughly related to the voltage v across the capacitance C_{gs} by

$$i = C_{\mathrm{gs}}\frac{\partial v}{\partial t}. \tag{15}$$

This is equivalent to saying that the positive feedback is small in steady state. Using (13) in (14), we obtain

$$\frac{L\,di}{dt}+(R_T-R_{\text{in0}}+m_{\text{in}}v^2)i+\frac{1}{C_T}\int i\,dt=0 \qquad (16)$$

and the circuit equation of the oscillator can be formed by substituting (15) into (16) to obtain

$$\frac{d^2v}{dt^2}-\frac{R_{\text{in0}}-R_T}{L}\left(1-\frac{3m_{\text{in}}v^2}{R_{\text{in0}}-R_T}\right)\frac{dv}{dt}+\frac{v}{LC_T}=0. \qquad (17)$$

Letting $\alpha=(R_{\text{in0}}-R_T)/L$, $\gamma=3m_{\text{in}}/(R_{\text{in0}}-R_T)$, $\omega_0^2=1/LC_T$, and $x=v$, (17) becomes the VDP equation

$$\frac{d^2x}{dt^2}-\alpha(1-\gamma x^2)\,\frac{dx}{dt}+\omega_0^2x=0. \qquad (18)$$

The derivation has qualitatively shown that the voltages and currents of a transistor oscillator obey the VDP equation. The nonlinear input resistance is the saturating factor of the oscillator in this case. Even when the configuration of the oscillator changes, the form of the equation should remain the same. However, the detailed relationship between the VDP parameters and the oscillator parameter can be dramatically different. In (18), parameter α is the saturation coefficient or damping constant and ω_0 is the resonance frequency in the absence of dissipation or gain. The constant α is proportional to ω_0/Q [14], where Q is the Q factor of an oscillator. In the case of a high Q-factor resonator where the frequency-locking range of the oscillator $\Delta\omega\ll\omega_0$, the value of α is evidently much smaller than ω_0.

Clearly, VDP parameters can also be evaluated numerically using the circuit parameters given on the data sheet. However, the direct calculation of the VDP parameters from the large-signal transistor parameters has the following disadvantages. First, the calculated parameters are model dependent. Accurate models of the I–V curve and the nonlinear components of a transistor are required. Any error in one of these models will result in a different value of α and γ, which in turn will result in a false prediction of the coupled transistor performance. Second, the calculated VDP parameters are circuit dependent. Different configurations of the passive circuit structures will result in different types of relationships between them. Therefore, real-time measurements on an oscillator to obtain VDP parameters are more realistic. The real power of using a VDP equation comes not only from its reduced parameter space, but from the ability to quickly evaluate the parameters experimentally, providing a simple diagnostic tool.

III. Theory of Determining the VDP Parameters Experimentally

In Sections I and III, we have justified that self-sustained oscillation is governed by the VDP equation. It is known that there exists an analytical stationary solution of (18) under the condition that α is small, compared to ω_0, which is given by [24], [25]

$$x=\sqrt{\frac{2}{\gamma}}\cos\tau+\alpha\left(\frac{3}{4\omega_0\sqrt{\gamma}}\sin\tau-\frac{1}{4\omega_0\sqrt{\gamma}}\sin(3\tau)\right)+\cdots \qquad (19)$$

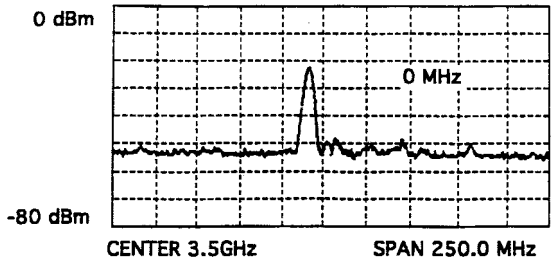

Fig. 6. Power spectrum of the transistor oscillator.

where

$$\tau=\omega_0 t\left(1-\frac{\alpha^2}{16\omega_0^2}+\cdots\right). \qquad (20)$$

Since α/ω_0 is small, the higher order terms of the solution can be neglected. The approximate stationary solution for force-free oscillation is

$$x=\sqrt{\frac{2}{\gamma}}\cos(\omega_0\tau). \qquad (21)$$

With a high-Q resonator, an oscillation frequency of the VDP oscillators is close to the resonant frequency ω_0. The amplitude of the oscillation is inversely proportional to the square root of parameter γ. The oscillation frequency and the magnitude of a VDP oscillator can both be obtained from a measurement using a spectrum analyzer. Therefore, the parameter γ can be determined experimentally. Fig. 6 shows the spectrum of a self-oscillating active antenna. We can see that the second-order and higher order terms of the steady-state solution in (21) are too small to be detected by the spectrum analyzer. This is further proof that the active antenna is a VDP oscillator and has small values of α/ω_0.

Notice that the stationary solution of the VDP equation in (21) only gives information about the parameter γ, but has no information about the absolute value of α/ω_0. If one wants to determine all of the VDP parameters experimentally, one needs another measurement. Since the constant α is proportional to ω_0/Q, the relative value of α can be estimated from measuring the locking bandwidth of the oscillator. Calibration of a locking measurement can be a problem. Here, we will consider another technique.

The technique we propose in the following derivation can be used to complete the parameter determination. In this approach, we add an external sinusoidal signal with frequency ω_f to the original bias voltages of a self-sustained transistor oscillator. Thus, the formulation which corresponds to the VDP equation can be described as follows:

$$\frac{d^2x}{dt^2}-\alpha(1-\epsilon\cos(\omega_f t))(1-\gamma x^2)\,\frac{dx}{dt}+\omega_0^2x=0. \qquad (22)$$

The VDP equation with constant coefficients has been treated by many researchers [12], [14], [24], [25]. However, to our knowledge, the solution of (22) is not available in any of the previous studies of the VDP equation. As we know, there is no simple closed-form expression for such a nonlinear oscillation, but it is possible for one to try to obtain the approximate solution of the differential equations under certain conditions.

In this section, we will use a multiple-scale expansion method to analyze (22) and to predict what will be measured by a spectrum analyzer. Furthermore, we will explain how to extract the parameters from the measurement. Again, this approach is used under the assumption that α/ω_0 is much smaller than one. The comprehensive treatment of this type of stationary oscillation is shown as follows. Using the method of multiple scales [24], we introduce new independent variables according to

$$T_n = \epsilon^n t, \qquad n = 0, 1, 2, \cdots. \tag{23}$$

It follows that the derivatives with respect to t in terms of the partial derivatives with respect to T are related by

$$\frac{d}{dt} = \frac{\partial}{\partial T_0}\frac{dT_0}{dt} + \frac{\partial}{\partial T_1}\frac{dT_1}{dt} + \cdots = D_0 + \epsilon D_1 + \cdots \tag{24}$$

and

$$\frac{d^2}{dt^2} = D_0^2 + 2\epsilon D_0 D_1 + \cdots \tag{25}$$

where

$$D_n = \frac{\partial}{\partial T_n}, \qquad n = 0, 1, 2, \cdots. \tag{26}$$

Taking ϵ^0 and ϵ^1 as the first-order approximations, we seek an approximate solution of (22) in the form

$$x(t, \epsilon) = x_0(T_0, T_1) + \epsilon x_1(T_0, T_1) + \cdots. \tag{27}$$

Substituting (27) through first order into (22), we have

$$\frac{d^2x_0}{dt^2} + \epsilon\frac{d^2x_1}{dt^2} + \omega_0^2 x_0 + \epsilon\omega_0^2 x_1 = \alpha(1+\epsilon\cos(\omega_f t))(1-\gamma(x_0+\epsilon x_1)^2)\left(\frac{dx_0}{dt} + \epsilon\frac{dx_1}{dt}\right). \tag{28}$$

Transforming the derivatives and keeping the terms ϵ^0 and ϵ^1 only, the left and right terms of (28) become

$$\begin{aligned} &D_0^2 x_0 + \omega_0^2 x_0 + \epsilon(2D_0D_1x_0 + D_0^2x_1 + \omega_0^2 x_1) \\ &\quad = \alpha[(1-\gamma x_0^2)D_0x_0 + \epsilon(\cos(\omega_f t)D_0x_0 - 2\gamma x_0 x_1 D_0 x_0 \\ &\qquad + (1-\gamma x_0^2)D_1x_0 + (1-\gamma x_0^2)D_0x_1)]. \end{aligned} \tag{29}$$

Equating the coefficients of like powers, ϵ^0 and ϵ^1 on both sides (left and right terms) of (29), we have

$$D_0^2 x_0 - \alpha(1-\gamma x_0^2)D_0x_0 + \omega_0^2 x_0 = 0 \tag{30}$$

and

$$\begin{aligned} &D_0^2x_1 - \alpha(1-\gamma x_0^2)D_0x_1 + \omega_0^2x_1 + 2\gamma x_0x_1D_0x_0 \\ &\quad = \alpha[\cos(\omega_f t)D_0x_0 + (1-\gamma x_0^2)D_1x_0]. \end{aligned} \tag{31}$$

As was discussed earlier (19), the lowest order solution of (30) is given by (21). Now, (31) is a formidable equation to handle exactly, but this is not the idea behind perturbation theory. We need to expand (31) to a self-consistent first order. Using the solution of (21) for x_0, we note that (31) reduces to

$$D_0^2x_1 + \omega_0^2x_1 = -\sqrt{\frac{2}{\gamma}}\,\alpha\omega_0\cos(\omega_f t)\sin(\omega_0 t) \tag{32}$$

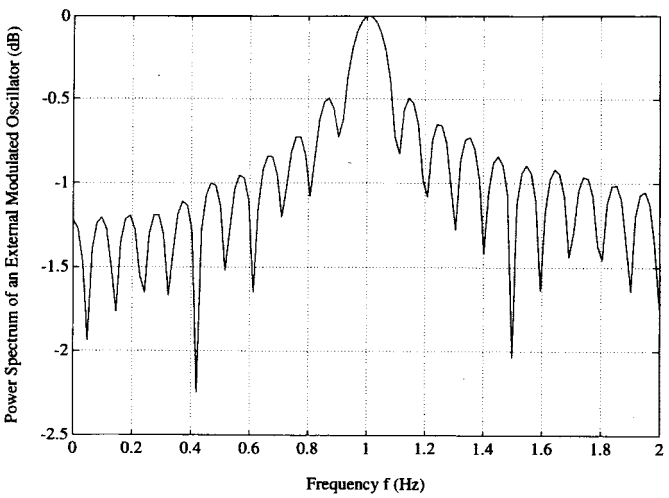

Fig. 7. Power spectrum of the VDP equation with a periodical coefficient calculated from a numerical simulation. Simulation parameters $\epsilon = 0.01$, $\gamma = 0.01$, $\omega_0 = 1$ Hz, and $\omega_f = 0.1$ Hz.

where terms like $(1-\gamma x_0^2)$ are zero to first order and terms like $x_1x_0^2$ were ignored. D_0^2 can be explained away as follows. To lowest order, we would like x_0 to vary with T_0 and x_1 to vary with T_1. Dependence of x_0 on T_1 and x_1 on T_0 should be weaker. The second derivative of x with respect to T_0 can indeed be seen to lead to terms at $2\omega_0$, which is counter to the multiple scales hypothesis. Ignoring this second derivative, we find that

$$x_1 = -\sqrt{\frac{1}{2\gamma}}\,\frac{\alpha}{\omega_0}[\sin((\omega_0+\omega_f)t) + \sin((\omega_0-\omega_f)t)] \tag{33}$$

where a trigonometric identity has been used, as has the fact that T_0 is just t. The first-order correction to the lowest order solution has added sidebands to the fundamental at an amplitude $\epsilon\alpha/2\omega_0$ [see (27)] below the fundamental. Successive corrections would add successive sidebands at angular frequencies $\omega_0 \pm n\omega_f$ with amplitudes proportional to coefficients multiplied by $(\epsilon\alpha/2\omega_0)^n$. We will see in Section IV that this is indeed the experimental result. Measurement of the first sideband and comparison with the theoretical result will be sufficient to determine the α, which is what we set out to do.

IV. Results and Discussion

We have now shown that the VDP damping factor α can be extracted by simply adding an external modulation frequency to an oscillator and measuring the relative amplitudes of the sidebands. Since the multiple-scales technique employed approximations in order to achieve the simple result shown in (33), it is necessary to verify the accuracy of the approximate solution. The results from the direct numerical calculation of (22) are compared with the analytical solution obtained by the method of multiple scales. Fig. 7 shows the power spectrum of a direct numerical solution in the frequency domain. For convenience in calculation, a low frequency of operation is employed. The resonant frequency ω_0, used in the simulation is 1 Hz, and the external modulation frequency ω_f is 0.1 Hz. What is important is not really these absolute values, but their ratio. What we are assuming is that the modulation frequency

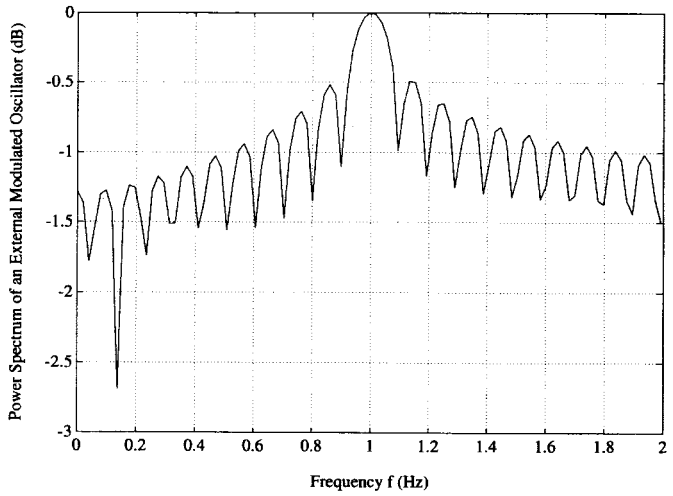

Fig. 8. Power spectrum of the VDP equation with a periodical coefficient calculated from analytical solution. Simulation parameters $\epsilon = 0.01$, $\omega_0 = 1$ Hz, and $\omega_f = 0.1$ Hz.

is being applied at 10% of the oscillation frequency. As we will see, in the experiment we perturbed at a frequency which corresponds to a significantly smaller ratio to the center frequency (roughly 0.1%) compared to the 10% in the simulation, but we used comparable amplitudes in simulation and experiment. To solve the simulation equation for $\omega_f \ll \omega_0$ requires a time proportional to ω_0/ω_f. This is the reason for the 10% instead of 0.1%. The important thing to compare between simulation and experiment will be the number of sidebands for a given amplitude of perturbation, as the distance of the sidebands from the center of the line is seen to scale with the ω_f for $\omega_f < \omega_0$. When $\omega_f \to \omega_0$, other instabilities could be observable. In the numerical calculation, (22) is converted into a set of nonlinear first-order differential equations, and these are then solved numerically in the time domain. The power spectrum of the solution is obtained by discrete fast Fourier transform. From Fig. 7, one should see that the center frequency of the oscillation is close to the resonant frequency of the circuit ω_0. As expected, many sidebands are generated from the external modulation frequency ω_f, and the frequency displacement of the sidebands from the center frequency is $\pm n\omega_f$. Thus, there are nine sidebands in the frequency range of 1 Hz, as shown in the plot. Fig. 8 shows the power spectrum of the approximate solution of (22) derived from the method of multiple scales. Comparing Fig. 8 with Fig. 7, reasonable agreement with the direct numerical calculation is observed. In particular, the magnitudes of the first and second sidebands from the two calculations are in better agreement than the higher order sidebands. The error in the higher order sidebands mainly originates from the neglect of the higher order terms in the approximate solution. Results of Figs. 7 and 8 indicate that (33) provides an accurate approximate solution for practical application.

The experimental setup used to verify the theory is shown in Fig. 9. The transistor is biased with two independent power supplies: the drain–source terminal is connected to a dc power supply, and the gate–source terminal is connected to a signal generator. As the transistor starts oscillation, the output power

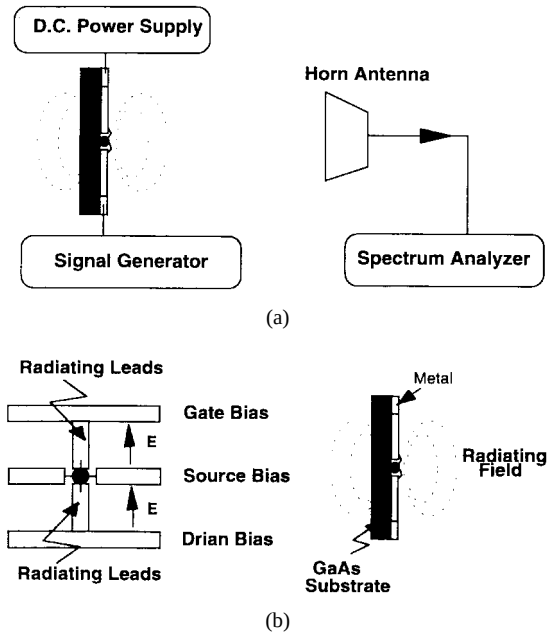

Fig. 9. (a) Experimental setup for a measurement of the VDP parameter. (b) A structure of the active antenna in the front view and the side view.

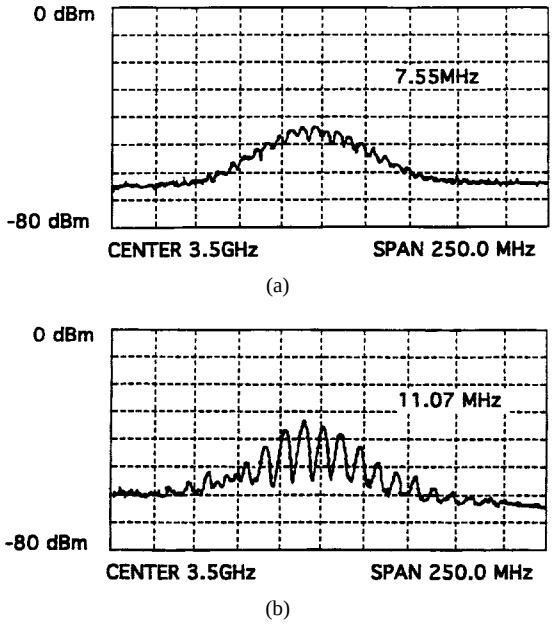

Fig. 10. Power spectra of a self-sustained active antenna at different external modulation frequencies. Center oscillation frequency $\omega_0 = 3.5$ GHz. (a) $\omega_f = 7.5$ MHz. (b) $\omega_f = 11.07$ MHz.

of the active antenna is detected by a horn antenna about 35 cm away. This signal is fed to a spectrum analyzer. With only dc-bias voltages used, the VDP parameter γ can be determined by using (21) with the measurement data of Fig. 6. When a modulated signal is added to the gate–source bias voltage of the transistor, the power spectrum of the oscillator is shown in Fig. 10(a) and (b), where modulated frequencies ω_f are 7.5 and 11.07 MHz, respectively. As the frequency ω_f increases, the displacement of sidebands from the center frequency increases, and the frequency offsets are exactly in the form of $\omega_0 \pm n\omega_f$. These phenomena are in agreement with those predicted from our theory. By measuring the ratio of the magnitude of the first sideband to the fundamental, the

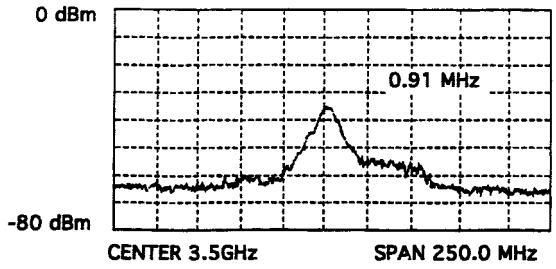

Fig. 11. Power spectrum of a self-sustained active antenna with external modulation frequency $\omega_f = 0.91$ MHz, which is less than the bandwidth of the phase noise.

value of α can be calculated from (27) and (33).

It is important to note that when we solved (22), which is in the form of

$$\frac{d^2x}{dt^2} - \alpha(1+\epsilon\cos(\omega_f t))(1-\gamma x^2)\frac{dx}{dt} + \omega_0^2 x = F_n(t) + F_{\text{ext}}(t) + \cdots \quad (34)$$

where $F_n(t)$ are noise terms and $F_{\text{ext}}(t)$ can be an external injection-locking signal, etc., we considered the equation to be source-free. That is, the terms in the right side of the equation are set to zero. Therefore, the linewidth of the spectrum calculated from the approximation solution is zero. Theoretically, the VDP parameter ϵ can be determined from the experiment as long as the modulation frequency ω_f is larger than zero. However, practically speaking, the transistor oscillator is not noise-free, and the spectrum of the oscillator has a certain spectral width. It is well-known that GaAs MESFET's have excess low-frequency noise at frequencies below 10 kHz due to trapped electrons in the semi-insulating substrate. These deeply trapped electrons cause dc current fluctuations in the source-drain channel and, hence, introduce noise to the oscillator. The behavior of this type of noise will decrease as $f^{-3/2}$ above 10 kHz [26], [27]. This $f^{-3/2}$-like noise is the fundamental noise in GaAs field-effect transistors. If the noise source is considered in the VDP equation, the phase of the oscillation of the transistor oscillator will have a time-dependent term, which we call the phase noise of the oscillator. The linewidth of the oscillator is directly proportional to the bandwidth of the phase noise. Therefore, if the external modulation frequency ω_f is less than the linewidth of the oscillator, the result of the external modulation in the bias line will be only to broaden the linewidth of the VDP oscillator, and the multiple spectra cannot be resolved from the measurement (shown in Fig. 11). It is recommended that the modulation frequency of ω_f be larger than 1 MHz for this proposed experiment. As another example, a radiating structure similar to the one shown in Fig. 9(b) was fabricated on Duroid to determine the accuracy of (33). The fundamental frequency of operation was around 2.54 GHz, and external modulations of 3 and 4 MHz were used, respectively. Fig. 12(a) and (b) show the sideband structure when external modulation is added. It was observed, however, that if an oscillator has multiple oscillations, then the beatnote of the external modulation with the higher oscillation frequencies can interfere with the accuracy of this measurement technique. Therefore, it is necessary that the oscillator be a single-frequency oscillator.

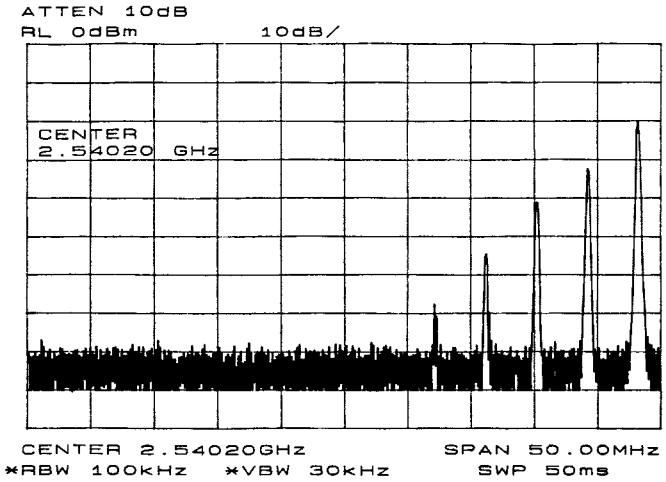

(a)

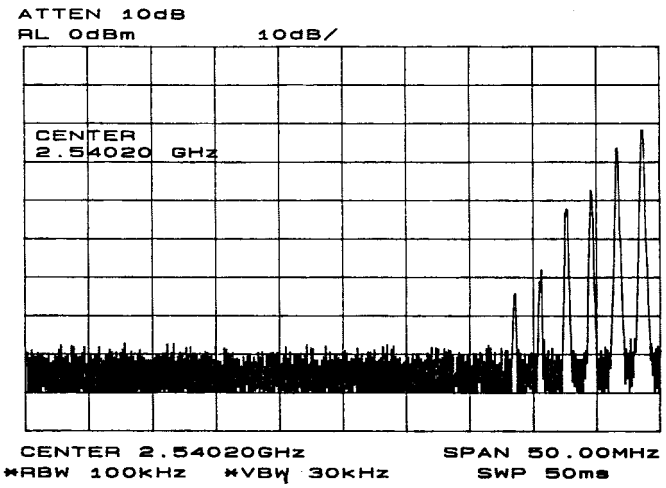

(b)

Fig. 12. Power spectra of a self-sustained active antenna at different external modulation frequencies constructed on Duroid. Center oscillation frequency $\omega_0 = 2.54$ GHz. (a) $\omega_f = 3$ MHz. (b) $\omega_f = 4$ MHz.

V. Summary

We have shown that the operation of a transistor oscillator can be described by the VDP oscillator equation. We have demonstrated that the VDP parameters are directly related to the circuit parameters of an oscillator. By applying an external modulated signal to the bias voltage of a transistor oscillator, a simple approach to determine the VDP parameters from the experiment has been developed. Analysis of the time dependence of the response of a modulated oscillator indicates that the magnitude of the spectral sidebands, which the response of the oscillator develops, are strongly dependent on the VDP parameters. An analytical expression to determine both of the VDP parameters from such an experiment are given. Results of the experiment agree with the theoretical predictions, which further justifies the perturbation theory. The procedure can be summarized as follows. *Step 1*: The power spectrum of an oscillator under normal bias voltages is

measured. By measuring the amplitude of the oscillation, the parameter γ can be calculated from (21). *Step 2*: A sinusoidal modulated signal is added to one of the bias voltages of the oscillator. By measuring the amplitude of the main peak and first sideband, the damping parameter α can be obtained with use of (33). Comparing the amplitude of the main oscillation frequency in Step 2 with the one in Step 1, the effect of the modulation depth can be calibrated. Notice that this technique is only valid for an oscillator with a single oscillation frequency. The VDP oscillator model has advantages for predicting the dynamic behavior of an oscillator under the influence of external injection signals and for analysis of coupled oscillator arrays. If one needs to use the VDP equation for a transistor oscillator, the presented technique provides an alternative and effective means to determine the VDP parameters experimentally.

REFERENCES

[1] W. R. Curtice, "A MESFET model for use in the design of integrated circuits," *IEEE Trans. Microwave Theory Tech.*, vol. MTT-28, pp. 448–456, May 1980.

[2] W. R. Curtice and M. Ettenberg, "A nonlinear GaAs FET model for use in the design of output circuits for power amplifiers," *IEEE Trans. Microwave Theory Tech.*, vol. MTT-33, pp. 1383–1394, Dec. 1985.

[3] W. R. Curtice, "GaAs FET modeling and nonlinear CAD," *IEEE Trans. Microwave Theory Tech.*, vol. 36, pp. 220–230, Feb. 1988.

[4] Y. Hu, J. Obregon, and J. Mollier, "Nonlinear analysis of microwave FET oscillators using Volterra series," *IEEE Trans. Microwave Theory Tech.*, vol. 37, pp. 1689–1693, Nov. 1989.

[5] M. Miller, M. Golio, B. Bechwith, E. Arnold, D. Halchin, S. Ageno, and S. Dorn, "Choosing an optimum large-signal model for GaAs MESFET's and HEMT's," in *IEEE Microwave Theory Tech. Symp. Dig.*, Dallas, TX, 1990, pp. 1279–1282.

[6] I. Smith, "Dynamic modeling of nonlinear microwave devices," *Electron. Lett.*, vol. 25, pp. 1237–1239, Aug. 1989.

[7] A. Madjar, "A fully analytical ac large-signal model of the GaAs MESFET for nonlinear network analysis and design," *IEEE Trans. Microwave Theory Tech.*, vol. 36, pp. 61–67, Jan. 1988.

[8] H. S. Statz, P. Newman, I. Smith, R. A. Pucel, and H. Haus, "GaAs FET device and circuit simulation in SPICE," *IEEE Tran. Electron Devices*, vol. ED-43, pp. 160–169, Feb. 1987.

[9] V. Rizzoli, C. Cecchetti, A. Lipparini, and F. Mastri, "General-purpose harmonic balance analysis of nonlinear microwave circuits under multitone excitation," *IEEE Trans. Microwave Theory Tech.*, vol. 36, pp. 1650–1660, Dec. 1988.

[10] J. M. Dortu and J. E. Muller, "Accurate large-signal GaAs MESFET modeling for a power MMIC amplifier design," *Microwave J.*, vol. 36, pp. 74–84, Apr. 1993.

[11] Z. B. Popovic, R. M. Weikle, M. Kim, and D. B. Rutledge, "A 100-MESFET planar grid oscillator," *IEEE Trans. Microwave Theory Tech.*, vol. 39, pp. 193–200, Feb. 1991.

[12] B. Van der Pol, "Forced oscillations in a system with nonlinear resistance," *Philos. Mag.*, vol. 3, pp. 65–80, Jan. 1927.

[13] M. Sargent, M. O. Scully, and W. E. Lamb, Jr., *Laser Physics.* Reading, MA: Addison-Wesley, 1974.

[14] J. J. Stoker, *Nonlinear Vibrations in Mechanical and Electric Systems.* New York: Wiley, 1950.

[15] C. Hayashi, *Nonlinear Oscillations in Physical Systems.* New York: McGraw-Hill, 1964.

[16] K. Kurokawa, "Some basic characteristics of broadband negative resistance oscillator circuits," *Bell Syst. Tech. J.*, vol. 48, pp. 1937–1955, July/Aug. 1969.

[17] R. Adler, "A study of locking phenomena in oscillators," *Proc. IRE*, vol. 34, pp. 351–357, June 1946.

[18] R. A. York, "Nonlinear analysis of phase relationship in quasi-optical oscillator arrays," *IEEE Trans. Microwave Theory Tech.*, vol. 41, pp. 1799–1809, Oct. 1993.

[19] J. M. Golio, *Microwave MESFET's and HEMT's.* Norwood, MA: Artech House, 1991.

[20] R. Anholt, "Investigation of GaAs MESFET equivalent circuit using transient current-continuity equation solutions," *Solid State Electron.*, vol. 34, pp. 693–700, July 1991.

[21] L. J. Sevin, Jr., *Field-Effect Transistors.* New York: McGraw-Hill, 1965.

[22] K. Y. Chen, P. D. Biernacki, S. Buchheit, and A. R. Mickelson, "Non-invasive experimental determination of charge and voltage distributions on an active surface," *IEEE Trans. Microwave Theory Tech.*, vol. 44, pp. 1000–1009, July 1996.

[23] K. Chang, *Microwave Solid-State Circuits and Applications.* New York: Wiley, 1994.

[24] A. H. Nayfeh and D. T. Mook, *Nonlinear Oscillations.* New York: Wiley, 1979.

[25] N. Minorsky, *Nonlinear Oscillations.* New York: Wiley, 1950.

[26] J. Day, M. Trudeau, P. Maclister, and C. M. Hurd, "Instability and gate voltage in GaAs metal-semiconductor field-effect transistors," *Can. J. Phys.*, vol. 67, pp. 238–241, Apr. 1989.

[27] B. K. Ridley, J. J. Criso, and F. Shishiyanu, "Slow domains and negative resistance via the enhanced capture of transferred electrons in n-type GaAs," *J. Phys. C, Solid State Phys.*, vol. 5, pp. 187–198, Jan. 1972.

Kuang Yi Chen received the B.S. and M.S. degrees in mechanical engineering from South China Institute of Technology, China, in 1982 and 1986, respectively, the M.S. degree in control system from Idaho State University, Pocatello, in 1989, and the Ph.D. degree in electrical engineering from the University of Colorado, Boulder, in 1994.

From 1994 to 1996, she was a Design Engineer for the Storage Technology Corporation, where she was involved with development of high-speed and high-density magnetic recording devices. In 1996, she joined Aztek Engineering Inc., Boulder, CO, as Senior Electrical Engineer. She has been involved with the design and development of high-speed digital analog systems for telecommunication and medical applications. Her interests are in designing fiber-optical devices, electrooptical interface circuits, and high-speed digital systems.

Paul D. Biernacki was born in New Orleans, LA, in 1966. He received the B.S. degree (*summa cum laude*) in physics from Louisiana Tech University, Ruston, in 1989, and the M.S. and Ph.D. degrees from the University of Colorado, Boulder, in 1993 and 1996, respectively, both in electrical engineering.

During his career at the University at Colorado, his research has focused on computer-generated holography, spatial light modulators, microwave optics, and electrooptic sampling for defect recognition in semiconductor materials. He is currently working in the Microwave Photonics Section, Naval Research Laboratory, Washington, DC, where he is conducting research on photonic phased-array radar systems as well as fiber-optic systems technology including optical-microwave frequency conversion techniques.

A. Lahrichi, photograph and biography not available at the time of publication.

Alan Mickelson (S'72–M'78–SM'92) was born in Westport, CT, on May 2, 1950. He received the B.S.E.E. degree from the University of Texas, El Paso, in 1973, and the M.S. and Ph.D. degrees from the California Institute of Technology, Pasadena, in 1974 and 1978, respectively.

Following a post-doctoral period at Caltech in 1980, he joined the Electronics Research Laboratory, Norwegian Institute of Technology, Trondheim, Norway, initially as an NTNF Post-Doctoral Fellow, and then as a Staff Scientist. His research in Norway primarily concerned characterization of optical fibers and fiber-compatible components and devices. In 1984, he joined the faculty of the Electrical and Computer Engineering Department, University of Colorado, Boulder, where, in 1986, he became an Associate Professor. His current research involves semiconductor laser characterization, integrated optic-device fabrication and characterization, fiber system characterization, and microwave/millimeter-wave devices.